

Journal Pre-proofs

A Novel Potent Metal-binding NDM-1 Inhibitor was Identified by Fragment Virtual, SPR and NMR Screening

Huifang Guo, Kai Cheng, Yan Gao, Weiqi Bai, Cai Wu, Wei He, Conggang Li, Zhuorong Li

PII: S0968-0896(20)30247-9
DOI: <https://doi.org/10.1016/j.bmc.2020.115437>
Reference: BMC 115437

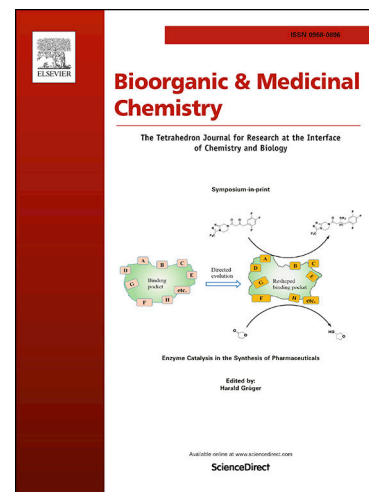
To appear in: *Bioorganic & Medicinal Chemistry*

Received Date: 26 January 2020
Revised Date: 5 March 2020
Accepted Date: 10 March 2020

Please cite this article as: H. Guo, K. Cheng, Y. Gao, W. Bai, C. Wu, W. He, C. Li, Z. Li, A Novel Potent Metal-binding NDM-1 Inhibitor was Identified by Fragment Virtual, SPR and NMR Screening, *Bioorganic & Medicinal Chemistry* (2020), doi: <https://doi.org/10.1016/j.bmc.2020.115437>

This is a PDF file of an article that has undergone enhancements after acceptance, such as the addition of a cover page and metadata, and formatting for readability, but it is not yet the definitive version of record. This version will undergo additional copyediting, typesetting and review before it is published in its final form, but we are providing this version to give early visibility of the article. Please note that, during the production process, errors may be discovered which could affect the content, and all legal disclaimers that apply to the journal pertain.

© 2020 Elsevier Ltd. All rights reserved.



A Novel Potent Metal-binding NDM-1 Inhibitor was Identified by Fragment Virtual, SPR and NMR Screening

Huifang Guo^{a, 1}, Kai Cheng^{b, 1}, Yan Gao^a, Weiqi Bai^a, Cai Wu^c, Wei He^c, Conggang Li^{b, **}

Zhuorong Li^{a, *}

^a Institute of Medicinal Biotechnology, Chinese Academy of Medical Science and Peking Union Medical College, Beijing 100050, China.

^b Key Laboratory of Magnetic Resonance in Biological Systems, State Key Laboratory of Magnetic Resonance and Atomic and Molecular Physics, National Center for Magnetic Resonance in Wuhan, Wuhan Institute of Physics and Mathematics, Chinese Academy of Sciences, Wuhan 430071, China.

^c School of Pharmaceutical Sciences, Tsinghua University, Beijing 100084, China.

¹ These authors contributed equally to this work.

* Corresponding author.

** Corresponding author.

E-mail addresses: lizhuorong@imb.pumc.edu.cn (ZR Li), conggangli@wipm.ac.cn (CG Li).

Abbreviations used. NDM-1, New Delhi Metallo-1; SPR, surface plasmon resonance; NMR, nuclear magnetic resonance; MBP, metal-binding pharmacophore; MBL, metallo- β -lactamase; FBDD, fragment-based drug discovery; PDB, Protein Data Bank; CNCL PKU, Chinese National Compound Library of Peking University; LE, ligand efficiency; Hepes, 2-(4-(2-hydroxyethyl)-1-piperazinyl)-ethansulfonic acid; RU, response unit; DMSO, dimethyl sulfoxide.

Abstract

NDM-1 can hydrolyze nearly all available β -lactam antibiotics, including carbapenems. NDM-1 producing bacterial strains are worldwide threats. It is still very challenging to find a potent NDM-1 inhibitor for clinical use. In our study, we used a metal-binding pharmacophore (MBP) enriched virtual fragment library to screen NDM-1 hits. SPR screening helped to verify the MBP virtual hits and identified a new NDM-1 binder and weak inhibitor **A1**. A solution NMR study of ^{15}N -labeled NDM-1 showed that **A1** disturbed all three residues coordinating the second zinc ion ($\text{Zn}2$) in the active pocket of NDM-1. The perturbation only happened in the presence of zinc ion, indicating that **A1** bound to $\text{Zn}2$. Based on the scaffold of **A1**, we designed and synthesized a series of NDM-1 inhibitors. Several compounds showed synergistic antibacterial activity with meropenem against NDM-1 producing *K. pneumoniae*.

Keywords

NDM-1, metal-binding pharmacophore, fragment-based drug design, SPR, NMR

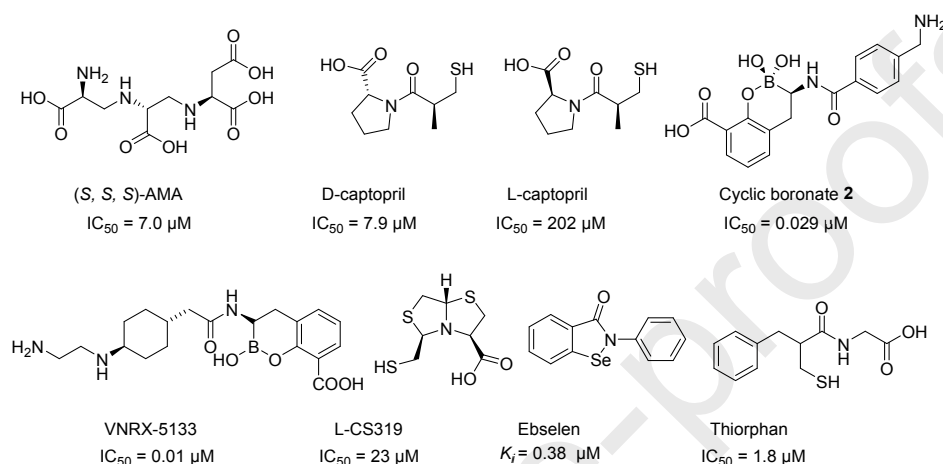
1. Introduction

The problem of antimicrobial resistance (AMR) becomes disturbing more than ever [1, 2]. According to WHO priority pathogens list for R&D of new antibiotics [3, 4], carbapenem-resistant *Acinetobacter baumannii*, *Pseudomonas aeruginosa* and *Enterobacteriaceae* are the highest ranked bacteria and regarded as a global priority for discovering new drugs.

Carbapenems, among the most used β -lactam antibiotics worldwide, are the most effective antibiotics against both Gram-positive and Gram-negative bacteria. Since carbapenems are highly effective against many bacterial species, less vulnerable to most β -lactam resistance determinants and safer to use than last-line resort polymyxins, they are considered the most reliable last-resort treatment for intractable infections [5-7]. Thus, the spread of carbapenem resistance poses a substantial threat to global morbidity and mortality.

The most challenging carbapenem-resistance cause is metallo- β -lactamase (MBL) NDM-1 [8]. NDM-1 can hydrolyze nearly all available β -lactam antibiotics, including carbapenems. Since its characterization in 2009 [9], NDM-1 has become a world-wide problem conferring bacterial resistance to all β -lactam antibiotics, with the only exception of monobactams (i.e., aztreonam) [10]. However, monobactam antibiotics can be inactivated by serine β -lactamase (SBL) normally coproduced with NDM-1, thus expanding bacterial resistance. Several SBL inhibitors are available in therapy [11, 12]. Valuable progresses have been made in the structural, mechanistic information and even activity inhibition of NDM-1 (Scheme 1) [13-23]. It had been very challenging to find NDM-1 inhibitors for clinical use [10]. Recently, cyclic

boronate SBL and MBL inhibitor Taniborbactam (VNRX-5133, Scheme 1) is in phase 3 clinical development [24]. Drug combination of cefepime and VNRX-5133 showed potent *in vitro* activity against *Enterobacteriaceae* and *P. aeruginosa*, including cefepime-, meropenem-, or piperacillin-tazobactam-non-susceptible isolates. [25] VNRX-5133 also restored cefepime antibacterial activity in both NDM-producing recombinant strains of *E. coli* and in clinical isolates of *Enterobacteriaceae*. [26] It is promising to see that NDM-1 might not an intractable drug target.



Scheme 1. Structures of some reported NDM-1 inhibitors [10, 13, 14, 17-19, 21, 24].

There are two catalytic zinc ions (Zn1 and Zn2) in the active site of NDM-1 [13]. NDM-1 catalyzes the hydrolysis of β -lactam antibiotics by the mediation of the two zinc ions [15], which coordinate a nucleophilic hydroxide to hydrolyze the β -lactam ring. Thus, the discovery of zinc-binding scaffold probably can help us to find new NDM-1 inhibitors. In our study, by the analysis of virtual screening hits of NDM-1, we developed a metal-binding pharmacophore (MBP) enriched fragment library. Then we developed first amine coupling-based method to immobilize tag-free NDM-1 onto CM7 chip, which helped us to verify NDM-1 hits with SPR screen. Fragment **A1** was found as a new NDM-1 binder and weak inhibitor. A solution NMR study of ¹⁵N-labeled NDM-1 [16] found that **A1** disturbed all three residues coordinating catalytic Zn2 of NDM-1. **A1**'s perturbation to the residues only happened in the presence of zinc ion. This is in accordance with molecular docking result that **A1** binds to Zn2 in the active pocket of NDM-1. Based on the scaffold of **A1**, we designed and synthesized a series of NDM-1 inhibitors. Several compounds showed some synergistic antibacterial activity with meropenem against NDM-1 producing *K. pneumoniae*.

2. Results and discussion

2.1 Virtual screening and set up of metal-binding pharmacophore enriched fragment library

Several well-conducted virtual screening of inhibitors of NDM-1 have been reported and new NDM-1 inhibitors were found, including sulfonamides [27, 28], thiols [29], N-arylsulphonyl hydrazones [29], succinic acids [29], mercaptocarboxylate acids [29], natural products [30, 31] and so on [32, 33, 34]. In our study, we try to run the virtual screen to identify NDM-1 binding fragments with metal-binding pharmacophore.

We used two compound libraries. One library was purchased from Maybridge (Cambridge, UK) and consisted of 2,500 fragments (Maybridge Ro3 diversity fragment library). The other library was Chinese National Compound Library of Peking University (CNCL PKU) and consisted of about 120,000 compounds. The whole Maybridge Ro3 diversity fragment library was run virtual screening with NDM-1 (PDB code: 4hl2, chain A). For CNCL PKU, compounds with molecular weight range out of 150 ~ 350 Da were all filtered out. Then the structure diversity of fragments was maximized with Discovery Studio and the top 28,000 compounds were used to run virtual screening with NDM-1.

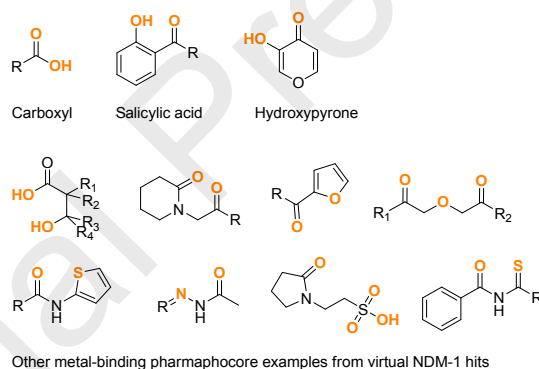
Virtual screening results first ranked the virtual fragment hits by total scores grading by Surflex-Dock of SYBYL-X2.0. The total scores of D- and L-captopril with NDM-1 calculated by Surflex-Dock were 5.9928 and 5.1273, respectively. Since in the docking by Surflex-Dock, the binding site is calculated as a rigid and inflexible site. More assays are needed to tell whether a virtual hit is a good hit. We then filtered the hits by whether they have metal-binding pharmacophores (MBPs). Some chemotypes are thought to be malleable MBPs to the binding of metalloenzymes, including picolinic acids, hydroxypyrones, hydroxylamines, salicylic acids and so on [35-37]. From the virtual hits with higher total score, we searched for compounds which had MBPs (Table 1, Scheme 2). Fingerprint module of Discovery Studio can help to filter and find the hits with specified MBP. High frequency of carboxyl groups was observed within high total score virtual hits from both CNCL PKU and Maybridge Ro3 (Table 1). However, other reported MBPs were rare. There are two possible reasons. One is that both compound libraries are not MBP rich. The other one is that many compounds with MBPs were not on our good virtual hit list. However, to enrich MBPs in our new filtered library for NDM-1 binding test with SPR, we manually checked virtual hits from CNCL PKU (with total score > 6.66) and Maybridge Ro3 (with total score > 5.0) to find more possible chemotypes.

Empirically, we selected 31 virtual fragment hits with other MBPs (Scheme 2) from CNCL PKU, which possibly could bind metal from the view of a chemist. We didn't find other MBPs than carboxyl group from virtual hits within Maybridge Ro3. At this point, we made the decisions only based on the chemical feature of fragments and didn't consider where the MBPs bound in NDM-1 active pocket. During the process of manual filtration of the virtual fragment hits, we kept some hits without any MBPs, since they have high total scores in virtual screening and passed further Lipinski rule [38] and Verber rule [39] filtration. Thus, we integrated an MBP enriched NDM-1 virtual fragment hits library. This library had 166 fragments from CNCL

PKU and 120 fragments from Maybridge Ro3 library (Table 1). In total, 286 fragments (50% fragments had MBP) were all tested by SPR to check whether they can bind to NDM-1 in solution.

Table 1. Metal-binding pharmacophore enriched NDM-1 virtual fragment hits library and NDM-1 binders identified by SPR.

Library size	Diversity fragments screened	Virtual fragment hits selected for NDM-1 binding test					NDM-1 fragment binders identified by SPR	
		Total 166 (166/28000 = 0.6%)					Priority I binders	Priority II binders
CNCL PKU 120,000	28,000	MBP					0 < K_D ≤ 1 mM	1 < K_D ≤ 2 mM
		Carboxyl	Salicylic acid	Hydroxypyrrone	Other	Not MBP		
		67	4	2	31	62		
Total MBP = 104 (104/166 = 63%)						41/166 = 25%		
Maybridge		Total 120 (120/2500 = 4.8%)					Priority I	Priority II
Ro3	2,500	MBP (Carboxyl was the only MBP)			Not MBP	18	15	
2,500		39 (39/120 = 33%)			81	18/120 = 15%		



Scheme 2. Metal-binding pharmacophores identified from NDM-1 virtual fragment hits in this study.

2.2 Identify NDM-1 binders by SPR screening

With the 286 fragments we got, we then investigated whether the hits that can bind to NDM-1 in solution by SPR. Sensitive biophysical techniques like SPR are well suited to identify protein fragment binders in fragment-based drug discovery, since functional assays are often not sensitive enough to detect the weak interaction between fragment and protein target [40].

Christopeit *et al* once described a SPR based biosensor assay for NDM-1 [41]. They immobilized the enzyme to the surface of a SPR sensor chip by biotin-streptavidin capturing

method and the immobilization level of NDM-1 was around 2,400 response units (RU). Their method required biotinylated NDM-1. We developed a new method to immobilize tag-free NDM-1 to CM7 SPR chip by establishing a covalent bond between amine group of N-terminal amino acid and the carboxyl group of CM7 chip. The immobilization level of NDM-1 reached more than 8,000 RU with our method, which might give higher responses during the screening of fragments. Real-time binding analysis of meropenem and L-captopril [10] to NDM-1 showed that the immobilized protein was active on CM7 chip (Figure 1).

Advantages of SPR screening also include that this method can realize medium to high through-put of screening and the initial amount of each virtual hit can be very low, as low as 5 μg each hit in our case. By the SPR method we developed, affinity screening was run to identify NDM-1 binders from MBP enriched hits library which included 120 fragments of Maybridge Ro3 library and 166 fragments purchased from CNCL PKU. The affinities of hits to NDM-1 were ranked according to the K_D s of fragments. We defined fragments with higher affinities ($0 < K_D \leq 1 \text{ mM}$) as priority I binders and hits with lower affinities ($1 < K_D \leq 2 \text{ mM}$) as priority II binders. In total, we got 41 priority I binders (hit rate = 25%) from CNCL PKU and 18 priority I binders (hit rate = 15%) from Maybridge Ro3 library (Table 1). It was not surprising that we got higher hit rate from CNCL PKU since the total scores of virtual hits we chose from the virtual screening were higher.

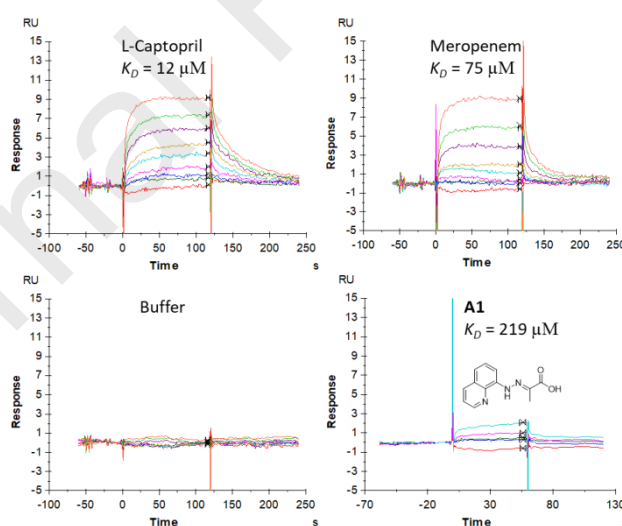


Figure 1. Binding sensorgrams of L-Captopril, meropenem, running buffer and compound **A1** dilutions. Tag-free NDM-1 coupled to CM7 chip by amine coupling can be used to screening fragment library. The affinities (K_D) of meropenem and **A1** were fit with the steady state affinity binding model. The affinity of L-Captopril was fit kinetics with 1: 1 binding model. The figures were generated by Biacore T200 evaluation software.

2.3 A solution NMR study of ^{15}N -enriched NDM-1 observed **A1**'s binding to Zn2 in the active

pocket

Solution-state NMR spectroscopy has proved to be a powerful technique to obtain atomic resolution structures of proteins and their complexes in solution [42, 43]. In contrast to X-ray crystallography, NMR provides an invaluable tool for studying weak fragment-protein complexes that are not amenable to crystallization. The x-ray structures of apo NDM-1 or complexes were reported [13, 15, 44]. In the current study, we titrated some of the NDM-1 priority I binders identified by SPR affinity screening into ^{15}N -labeled NDM-1 and utilized NMR spectra to identify the detail binding sites of priority I binders in NDM-1, according to our previous backbone chemical shift assignments [16].

A1 was an α -hydrazono carboxylic acid fragment (Figure 1). The affinity of **A1** to NDM-1 was 219 μM measured by SPR. We observed chemical shift perturbations (CSPs) in the ^1H - ^{15}N HSQC spectra of NDM-1 when titrated with priority I binder **A1** (Figure 2a). The chemical shifts of NDM-1 changed continuously as **A1** was added. Residues from Zn binding sites and active sites showed larger CSPs (Figure 2b). Molecular docking result showed that **A1** bound to the active pocket of NDM-1 and its carboxyl group coordinated to catalytic Zn2 in the pocket (Figure 3a). D124, C208 and H250 are the three residues coordinating Zn2 (Figure 3b). These residues showed larger CSPs than the residues coordinating Zn1 (H120, H122, H189) (Figure 2b) in NMR titration experiment, which confirmed the coordination of **A1** to Zn2. NMR titration experiment showed the affinity of **A1** to NDM-1 was 0.62 ± 0.02 mM based on the shift of D124 (Supplementary material). Within the three residues coordinating Zn1 (H120, H122, H189), only H122 was disturbed slightly. We also observed large CSPs of T119, V73, Q123 and L65 in the active sites, indicating these residues are also involved in the **A1** binding, which is consistent with the results of molecular docking.

We also noted that there was no CSPs of NDM-1 when titrated with **A1** after we removed all zinc ions from NDM-1 solution by dialysis (Figure S1). When two equivalents of zinc ions were added, the perturbation was restored (Figure S1). This observation further suggested that the interaction between **A1** and Zn2 was the major contribution of the binding and the carboxyl group of **A1** should be kept in further structure design and modification.

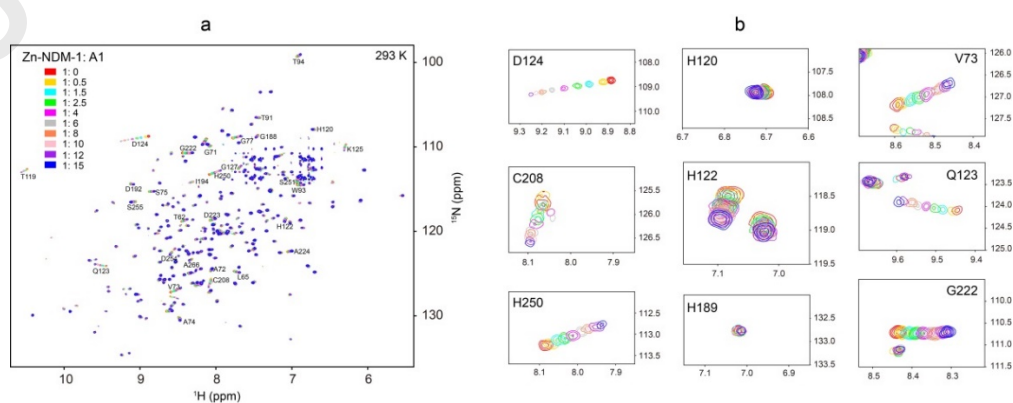


Figure 2. Compound **A1** disturbs the amino acid residues in NDM-1 active pocket. a: ^1H - ^{15}N HSQC spectra of di-Zn-NDM-1 titrated with **A1**. b: The expanded regions of ^1H - ^{15}N HSQC spectra of residues that located in Zn1 binding sites (H120, H122, H189), Zn2 binding sites (D124, C208, H250) and active sites (V73, Q123, G222).

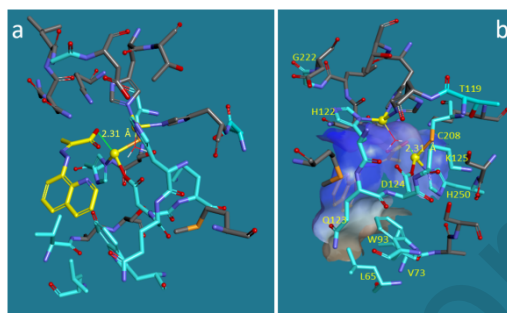
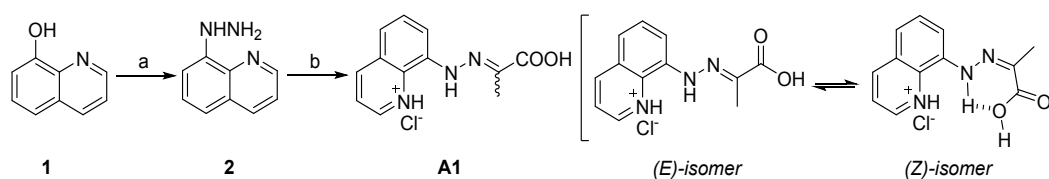


Figure 3. Molecular docking calculations of the binding modes of α -hydrazono carboxylic acids with NDM-1 (PDB code: 4hl2). The figures were prepared with Discovery Studio 2018. a: **A1** (yellow) was docked into the active pocket of NDM-1 and the **A1** carbonyl oxygen was found bind to catalytic zinc ion 2 (Zn2, yellow ball). b: Residues disturbed by **A1** binding (colored in blue) locate in NDM-1 active pocket. All of the three Zn2 coordinating residues (D124, C208 and H250) were disturbed, pointing to the existence of the binding **A1** to Zn2, not Zn1. Only one Zn1 coordinating residue (H122) was disturbed, and the disturbance is probably transmitted from the dramatic disturbance of D124.

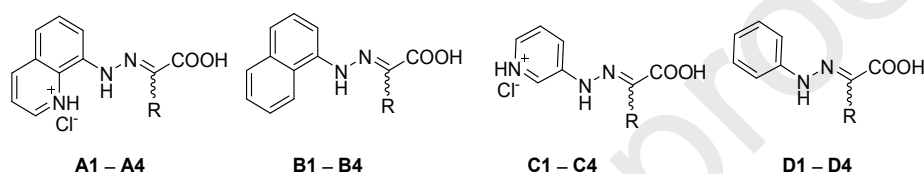
2.4 Design and synthesis of NDM-1 inhibitors

We synthesized **A1** by the route described in scheme 3 [45, 46] to carry on NMR and NDM-1 enzymatic inhibition tests. The NDM-1 enzymatic inhibition activity (IC_{50}) of fragment **A1** was $124.0 \pm 8.3 \mu\text{M}$ (Table 2). The parallel tests of an NDM-1 inhibitor L-captopril showed the enzymatic inhibitory activity of **A1** was stronger than L-captopril. L-captopril is an approved drug in the treatment of hypertension [47]. The thiol of L-captopril was found intercalating the two zinc ions of NDM-1 in the X-ray structure [15]. To get more potent NDM-1 inhibitors, we decided to design and synthesize new compounds based on the scaffold of **A1**. The carboxyl group of **A1** was the metal-binding pharmacophore coordinated to Zn2 of NDM-1 according to the NMR and molecular docking results. So, it was kept intact in the following design and syntheses. The newly designed compounds (Table 2) included changing the aryl rings and substituents of the α -position of the carboxyl group. We evaluated NDM-1 enzymatic inhibitory activities of the newly synthesized α -hydrazono carboxylic acids (Table 2). The compounds showed weak to moderate strong NDM-1 inhibiting activities.



Scheme 3. Synthesis of the hydrochloride of **A1**. Conditions and reagents: a) 80% hydrazine hydrate, reflux 10 h. 40% yield. b) CH₃COCOOH, HCl, H₂O, r.t., 2 h. 77% yield.

Table 2. Structures, IC₅₀ Values, NDM-1 binding affinities, and ALogPs of newly designed α -hydrazono carboxylic acids against NDM-1.



ID	R ^a	K _D (μM) ^b	IC ₅₀ (μM) ^c	ALogP ^d
A1	CH ₃	290.5 ± 177.4	124.0 ± 8.3	-0.545
A2	Et	275.1 ± 165.6	68.2 ± 19.9	0.122
A3	<i>n</i> -Pr	221.4 ± 63.0	82.3 ± 13.6	0.578
A4	<i>t</i> -Bu	435.0 ± 40.2	> 500	1.002
B1	CH ₃	255.2 ± 21.8	388.9 ± 191.0	2.439
B2	Et	449.4 ± 62.1	28.1 ± 41.1	3.106
B3	<i>n</i> -Pr	> 1000	> 500	3.562
B4	<i>t</i> -Bu	306.8 ± 93.3	94.6 ± 44.0	3.985
C1	CH ₃	> 1000	n. t.	-1.744
C2	Et	> 1000	n. t.	-1.077
C3	<i>n</i> -Pr	702.9 ± 185.9	n. t.	-0.621
C4	<i>t</i> -Bu	> 1000	n. t.	-0.198
D1	CH ₃	167.8 ± 54.5	n. t.	1.531
D2	Et	190.7 ± 153.4	n. t.	2.198
D3	<i>n</i> -Pr	187.7 ± 31.7	n. t.	2.654
D4	<i>t</i> -Bu	438.4 ± 187.6	n. t.	3.077
L-Captopril	--	14.1 ± 1.9	390.5 ± 87.6	0.667
EDTA-2Na	--	> 1000	17.2 ± 10.2	--

^a Et = ethyl, *n*-Pr = *n*-propyl, *t*-Bu = *tert*-butyl. ^b K_D values are collected from three separate tests tested by SPR. ^c IC₅₀ values are collected as the mean ± SD from three separate tests. ^d ALogP values were calculated with Discovery Studio 2018.

2.4 The NDM-1 inhibition and binding activity of synthesized α -hydrazono carboxylic acids.

The ability of synthesized α -hydrazono carboxylic acids to bind and inhibit NDM-1 were evaluated. From the binding affinity data, it was found that fragments with quinoline (**A1** – **A4**) naphthalene (**B1**, **B2**, **B4**) and benzene (**D1** – **D4**) rings showed medium to weak binding affinities to NDM-1 (Table 2). Compare the binding affinities of fragment **A1** – **A4** and **D1** – **D4**, it can be found that the R groups of methyl, ethyl and *n*-propyl contribute to the affinity similarly, while bulk *tert*-butyl substitution can decrease the affinity.

In NDM-1 inhibition tests of synthesized α -hydrazono carboxylic acids, nitrocefin is not a suitable chromogenic substrate, since inhibition effects were always observed at lower but not higher fragment concentrations in our tests. With meropenem as the chromogenic substrate, we observed evident NDM-1 inhibition by fragments **A2**, **A3** and **B2** (Table 2). Fragments with pyridine (**C1** – **C4**) and benzene (**D1** – **D4**) have absorption around 300 nm and NDM-1 inhibition data were not tested.

L-captopril is a strong binder but weak NDM-1 inhibitor. EDTA-2Na showed evident NDM-1 inhibiting activity by its well-known metal chelating property. However, EDTA-2Na didn't show obvious binding to NDM-1, possibly due to the lack of three-dimensional complementary with NDM-1's pocket. Compare the data of fragments **A1** – **A4** and **B1** – **B4**, most the affinities and IC₅₀s were correlated except **B2**, possibly influenced by the different tautomer in the tested condition.

2.5 The synergistic antibacterial activity of synthesized α -hydrazono carboxylic acids with meropenem against NDM-1 producing *K. pneumoniae*.

The ability of synthesized α -hydrazono carboxylic acids to restore the antibacterial activity of a clinically significant carbapenem antibiotic, meropenem, was assessed by performing MIC assays with *K. pneumoniae* (ATCC BAA-2470) cells expressing NDM-1. At the concentrations of 100 μ g/mL, compounds **A2**, **A4** and **B3** restored the meropenem MIC to 64, 64 and 32 μ g/mL.

We suppose that **A2** restore the meropenem MIC by binding and inhibiting NDM-1, since **A2** showed evident NDM-1 binding and inhibiting activities in the SPR and enzyme inhibitory tests (Table 1). In the NMR test, we observed the primary hit **A1** can disturb all three residues coordinating the Zn²⁺ in the active pocket of NDM-1 by binding Zn²⁺. The structure of **A1** and **A2** are very close. So, we also suppose that **A2** might inhibit NDM-1 by binding Zn²⁺ in *K. pneumoniae* (ATCC BAA-2470) cell. However, the synergistic antibacterial activity of **A2** was weak, mostly due to **A2** is a fragment, the binding and inhibiting activity need to be improved by more structure evolution. For the future optimization strategy, we suggest further designing based on the scaffold of **A2**. The carboxyl group of **A2** should be kept. If the imine group can be replaced with a carbon-carbon double bond, tautomerization can be avoided. Fragment grow at the quinoline ring may also can increase the affinity and potency of the scaffold. The outer

membrane of Gram-negative bacteria made most small molecules are harder to penetrate and accumulate inside the cell. Michelle et al [48, 49] reported that small molecules are most likely to accumulate with an amine group, are amphiphilic and rigid, and have low globularity. It is important to increase the accumulation inside the cell of the compounds.

Since compounds **A4** and **B3** didn't show evident affinity and inhibiting activities to NDM-1 (Table 1), we guess that their weak synergistic antibacterial activities are not due to NDM-1 inhibition.

Table 3. MICs of meropenem alone or in combination with α -hydrazono carboxylic acids (100 μ g/mL) against NDM-1 producing *K. pneumoniae* (ATCC BAA-2470).

Combination compounds	MICs (μ g/mL) of meropenem	Combination compounds	MICs (μ g/mL) of meropenem
A1	>64	C1	>64
A2	64	C2	>64
A3	>64	C3	>64
A4	64	C4	>64
B1	>64	D1	>64
B2	>64	D2	>64
B3	32	D3	>64
B4	>64	D4	>64
No combination	>64		

3. Conclusions

NDM-1 is a tough AMR factor that can inactivate almost all β -lactam antibiotics, even carbapenems. Discovery of potent NDM-1 inhibitors for clinical use is still very challenging. The zinc ions in the active site are essential for NDM-1's activity. The activity of NDM-1 can be inhibited by blocking the zinc ions. Metal binding has been a successful drug design strategy in the discovery of inhibitors of viral enzymes containing magnesium [35] and other metalloenzymes [50]. It is also optimistic to find drugs inhibiting NDM-1 through metal-binding. Fragment-based drug discovery strategy is very helpful to find NDM-1 inhibitors with metal-binding pharmacophore.

Our virtual screening of fragment library found primary NDM-1 virtual hits. By analysis and filtration of the virtual hits, we established a metal-binding pharmacophore enriched fragment library. Biophysical methods SPR and NMR then helped us to identify NDM-1 binders and the zinc ion binder **A1**. Based on the scaffold of **A1**, we designed and synthesized a series of potent NDM-1 inhibitors. Some showed synergistic antibacterial activity with meropenem in NDM-1 producing *K. pneumoniae*. By means of fragment MBP searching, it is promising to find more potent metal-binding NDM-1 inhibitors.

4. Experimental section

4.1 General information

All reagents and solvents were purchased and used without further purification unless specified. Virtual screening was performed with Surflex-Dock of SYBYL-X2.0. Molecular docking was calculated with CDOCKER of Discovery Studio 2018. TECAN (SPARK 20M) Plate Reader was used to measure absorbance in the NDM-1 enzymatic activity assay. Semi-preparative liquid chromatography was performed with Biotage Isolera One with a Biotage SNAP Cartridge KP-C18-HS 12 g column. Melting points of the compounds were observed with Mettler Toledo MP90 melting point system or Beijing Tech Instrument X-4 digital microscope melting point system. The ^1H NMR and ^{13}C NMR spectra of small compounds were recorded with a Bruker BioSpin GmbH spectrometer (400 MHz, 500 MHz or 600 MHz). The internal solvent residual peaks were used as references. The high-resolution mass spectra (HRMS) of small compounds were recorded on a Thermo Scientific LTQ Orbitrap XL with an ESI mass selective detector. NMR experiments of ^{15}N -labelled NDM-1 were carried out at 298 K and 293 K on a Bruker Avance 800 MHz spectrometer equipped with 5 mm triple-resonance HCN-cryoprobe.

4.2 NDM-1 expression and purification

NDM-1 was expressed according to the reported method [13]. Briefly, the NDM-1 gene was cloned into a pET-28a vector and the recombinant protein (residues I31 ~ K268) was expressed in *E. coli* strain BL21 (DE3) cells. *E. coli* BL21 (DE3) was transformed with recombinant plasmids. A single colony was inoculated into LB medium containing kanamycin (100 mg/L). Cultures were incubated in 37 °C at 200 rpm. IPTG (400 μM) was introduced for induction. Cells were allowed to grow for another 18–20 h at 22 °C and harvested. NDM-1 was obtained by three-step purification using Ni column, thrombin cleavage, Ni column and Superdex 200. Tag removal was performed to get the tag-free protein. Fractions were pooled and dialyzed followed by 0.22 μm filter sterilization. Proteins were analyzed by SDS-PAGE by standard protocols for molecular weight (27 kDa) and purity measurements (> 95%). Storage buffer of NDM-1 was 50 mM hepes (pH 7.5), 150 mM NaCl, 100 μM ZnCl_2 , 1 mM DTT.

4.3 ^{15}N -enriched NDM-1 expression and purification

^{15}N -enriched NDM-1 was expressed and purified according to the reported method [16].

Generally, the NDM-1 gene was cloned into a pET-21a vector and the recombinant protein (residue 36-270) contains a C-terminal His₆-tag (LEHHHHHH). The protein was expressed in *E. coli* strain BL21 (DE3) cells. Cells were grown in M9 media containing ¹⁵NH₄Cl at 37 °C and induced with 500 μM IPTG at 16 °C for 24 h when OD₆₀₀ reaching 0.8 to 0.9. Cells were harvested by centrifugation and resuspended in Ni-column buffer A (50 mM Tris, 500 mM NaCl, 10 mM imidazole, pH 7.5). Cells were lysed by sonication (JY92 IIN, 50% amplitude, 60 min, 37.5% duty cycle) on ice. The supernatant was collected after centrifugation at 16000 g at 4 °C for 30 min. NDM-1 was first purified using a prepacked Ni-NTA column (GE Healthcare), then followed by size exclusion chromatography (S100) with a buffer comprising 50 mM HEPES, 200 mM NaCl, pH 7.5. Proteins were assessed by SDS-PAGE. The concentration of NDM-1 was determined by using a molar extinction coefficient of 27960 M⁻¹ cm⁻¹ at 280 nm, which was calculated from the amino acid sequence using <http://web.expasy.org/protparam/>. For nonfunctional NDM-1 (apo-NDM-1), 20 equivalents of EDTA were added to the purified protein and the EDTA was soon removed by buffer exchange. For functional NDM-1 (di-Zn-NDM-1), two equivalents of Zn²⁺ were added to apo-NDM-1. The purified proteins were lyophilized and stored at -80 °C.

4.4 NMR spectroscopy

NMR titration experiments were carried out at 298 K and 293 K on a Bruker spectrometer operating at 800 MHz. NDM-1 were dissolved in 50 mM HEPES, 200 mM NaCl at pH 7.5. The concentration of ¹⁵N-enriched NDM-1 was 0.11 mM and 0.165 mM. All inhibitors were dissolved in DMSO with concentration of 20 mM and 50 mM. For the titrations of di-Zn-NDM-1 and apo-NDM-1 with **A1**, a series of ¹H-¹⁵N HSQC spectra were acquired. The NDM-1/inhibitor mole ratios varied from 1: 0 to 1: 0.5, 1: 1.5, 1: 2.5, 1: 4, 1: 6, 1: 8, 1: 10, 1: 12 and 1: 15 for **A1**. After apo-NDM-1 were titrated with inhibitors, two equivalents of Zn²⁺ were added to the solutions.

4.5 Affinity screening by SPR

SPR experiments were carried out using a Biacore T200 (GE Healthcare) at 25 °C. NDM-1 was preconditioned to 50 μg/ml in pH 5.0 sodium acetate and then immobilized to a CM7 chip by amine coupling. Running buffer was 100 mM Hepes (pH 7.5), 150 mM NaCl, 100 μM ZnCl₂, 0.005% P20 v/v. When the affinity screening of fragments was run, 2% DMSO was added to the buffer. Six concentrations of each fragment were used. Fragment concentration was diluted by two-fold serial dilution. Compounds were injected to the surface of the protein-coupled chip

channels at the flow rate of 30 $\mu\text{L}/\text{min}$. The affinities (K_D) were calibrated with the steady state affinity 1:1 binding model with the evaluation software of Biacore T200. The affinities of the fragments were tested once in SPR screen study.

In the binding study of synthesized α -hydrazono carboxylic acids (A1 ~ D4, in Table 2) to NDM-1, the running buffer was 10 mM Hepes (pH 7.5), 150 mM NaCl, 100 μM ZnCl_2 with 2% DMSO. EDTA-2Na was tested without DMSO in the buffer. Eight two-fold serial diluted concentrations of each compounds were tested. The affinities of compounds were tested at least three times.

4.6 NDM-1 Enzyme Inhibition Assay

NDM-1 enzymatic activity inhibition tests were carried on according to the reported method [21]. Briefly, the inhibitors were added to the NDM-1 (12 nM) and incubated for 20 min at room temperature. L-captopril was used as the parallel positive control. Then, the substrate (meropenem, 100 μM) was added. The final buffer contained 2% DMSO in 50 mM hepes (pH 7.24). Assays were performed in 96-well microplate format, and the absorbance was recorded at 300 nm using a TECAN plate reader (SPARK 20M) at 30 $^\circ\text{C}$. For each compound, two parallel wells were used. And the tests were replicated for three times. IC_{50}s were calculated from a plot of percent loss of activity versus inhibitor concentration with GraphPad InStat 3.

4.7 Virtual screening and molecular docking calculations

X-ray crystal structure of NDM-1 (PDB code 4hl2, chain A) was used for virtual screening and docking studies. The ligand was extracted from the catalytic active site of NDM-1 crystal structure, which was defined as binding site for virtual screening and docking calculations. Virtual screening was run with Surflex-Dock of SYBYL-X2.0. Chain A of 4hl2 (PDB code 4hl2) was used to prepare the protein. The ligand ampicillin in the co-crystal structure was extracted to define the docking site. The $\text{H}_2\text{O}701$ and two zinc ions were not kept when the other substructures were removed. Prepare the protein by adding hydrogens. Before virtual screening, all the fragments were energy minimized with max iterations of 2000, Tripos force field and Gasteiger-Huckel charges loading. CDOCKER of Discovery Studio 2018 was used to carry out the docking simulation of the compounds to NDM-1. Chain A of 4hl2 (PDB code 4hl2) was used to prepare the protein. Ampicillin-binding site was defined as the docking site with site sphere radius of 9. Ligands were prepared with the small molecule tool of Discovery Studio and fully minimized before docking. Ligands have two energy-minimized conformations. All the carboxyl groups of the top docking models showed coordination to $\text{Zn}2$. Ligands in *syn* conformation showed higher -CDOCKER energy score and was regarded as the

dominating pose.

4.8 Chemistry

General procedure for the syntheses of **A1**: as described in scheme 3, quinolin-8-ol (**1**, 2 g, 13.8 mmol) was added to 80% hydrazine hydrate (16 mL). The resulting mixture was heated to reflux and reacted for 10 h. The reaction was cooled to room temperature. To the reaction mixture, ~ 10 mL of 3M NaOH was added. Dichloromethane (20 mL) was then added to extract targeting material. Organic layer was washed with water and brine, and then dried over anhydrous MgSO_4 . Organic layer was collected by filtration and concentrated by rotary evaporator. The crude was then purified by silica column chromatography (petroleum ether: ethyl acetate = 10: 1 to 1: 1). 8-Hydrazinylquinoline (**2**) was then got as a brown solid (40% yield). ^1H NMR (400 MHz, CDCl_3) δ (ppm): 8.74 – 8.73 (m, 1H), 8.09 (d, 1H, $J = 8.4$ Hz), 7.46 (t, 1H, $J = 8.0$ Hz), 7.41- 7.38 (m, 1H), 7.17 (d, 1H, $J = 8.0$ Hz), 7.10 (d, 1H, $J = 7.6$ Hz).

8-Hydrazinylquinoline (**2**, 360 mg, 2.26 mmol) was added to 3 mL of water. HCl (240 μL) and a solution of 2-oxopropanoic acid (219 mg, 2.49 mmol) in water (0.4 mL) were added sequentially. Then the mixture was stirred for 2 h at room temperature. Filtrate to collect the yellow solid crude and wash the crude with water. Vacuum drying gave **A1** as a yellow solid (77% yield). Mp: 176.0 – 178.0 $^\circ\text{C}$. ^1H NMR (600 MHz, d_6 -DMSO) δ (ppm) (major isomer: (*E*)-isomer) 9.95 (s, 1H), 8.94 (dd, 1H, $J = 4.2$ Hz, 1.8 Hz), 8.54 (d, 1H, $J = 8.4$ Hz), 7.86 (dd, 1H, $J = 7.8$ Hz, 0.6 Hz), 7.71 (q, 1H, $J = 4.2$ Hz), 7.64 (t, 1H, $J = 7.8$ Hz), 7.57 (t, 1H, $J = 7.2$ Hz), 2.22 (s, 3H). ^{13}C NMR (150 MHz, d_6 -DMSO) δ (ppm) (major isomer: (*E*)-isomer) 165.92, 147.66, 138.42, 137.83, 136.48, 136.15, 128.39, 127.97, 122.17, 119.49, 108.25, 11.03. HRMS (ESI) calculated for $\text{C}_{12}\text{H}_{12}\text{N}_3\text{O}_2^+$ $[\text{M} + \text{H}]^+$ 230.0924, found 230.0922.

All the other compounds were synthesized with a similar procedure of the synthesis of **A1**. For targeting material need further purification, the purification was pursued with semi-preparative liquid chromatography (Biotage Isolera One). A Biotage SNAP Cartridge KP-C18-HS 12 g column with a gradient of 10 - 50% acetonitrile in water to was used. Lyophilization of the eluent gave respective products. The purities of all the compounds were above 95% (normalization method of peak area, see supporting information). The characterization data are as followed:

A2 is obtained as yellow solid (53% yield). Mp: 123 – 126 $^\circ\text{C}$. ^1H NMR (500 MHz, d_6 -DMSO) δ (ppm) (major isomer) 13.25 (s, 1H), 8.84 (d, $J = 2.5$ Hz, 1H), 8.32 (d, $J = 8.0$ Hz, 1H), 7.65 – 7.50 (m, 4H), 7.43 (d, $J = 8.0$ Hz, 1H), 2.55 (q, $J = 7.3$ Hz, 2H), 1.18 – 1.13 (m, 3H). ^{13}C NMR (101 MHz, d_6 -DMSO) (major isomer) δ 165.12, 148.95, 139.95, 138.72, 136.76,

136.57, 128.70, 127.92, 122.49, 119.02, 108.72, 27.01, 12.38. HRMS (ESI) calculated for $C_{13}H_{14}N_3O_2^+$ $[M + H]^+$ 244.1081, found 244.1072.

A3 is obtained as yellow solid (53% yield). Mp: 136.3 – 139.6 °C. 1H NMR (400 MHz, d_6 -DMSO) δ (ppm) (major isomer) 13.22 (s, 1H), 8.86 (d, $J = 2.8$ Hz, 1H), 8.34 (d, $J = 8.0$ Hz, 1H), 7.68 – 7.54 (m, 4H), 7.46 (d, $J = 8.0$ Hz, 1H), 1.68 – 1.69 (m, 2H), 1.02 – 0.95 (m, 3H). ^{13}C NMR (101 MHz, d_6 -DMSO) (major isomer) δ 164.55, 148.57, 139.32, 136.15, 132.52, 128.23, 127.45, 122.07, 118.78, 110.23, 108.38, 35.18, 20.52, 13.69. HRMS (ESI) calculated for $C_{14}H_{16}N_3O_2^+$ $[M + H]^+$ 258.1237, found 258.1241.

A4 is obtained as yellow solid (53% yield). Mp: 135.6 – 138.9 °C. 1H NMR (500 MHz, d_6 -DMSO, *Z*) δ (ppm) 12.51 (s, 1H), 8.84 (s, 1H), 8.33 (d, $J = 8.2$ Hz, 1H), 7.66 – 7.50 (m, 3H), 7.44 (d, $J = 7.9$ Hz, 1H), 1.33 (s, 9H). ^{13}C NMR (101 MHz, DMSO) δ 164.95, 148.94, 140.50, 140.15, 136.78, 136.61, 128.65, 127.94, 122.50, 118.93, 108.91, 37.51, 29.24. HRMS (ESI) calculated for $C_{15}H_{18}N_3O_2^+$ $[M + H]^+$ 272.1394, found 272.1382.

B1 is obtained as yellowgreen solid (10% yield). Mp: 146.6 – 149.3 °C. 1H NMR (400 MHz, d_6 -DMSO) δ (ppm) (major isomer) 12.20 (br s, 1H), 9.52 (s, 1H), 8.30 (dd, $J = 5.9, 3.1$ Hz, 1H), 7.89 (dd, $J = 5.9, 3.0$ Hz, 1H), 7.66 (d, $J = 7.3$ Hz, 1H), 7.59 – 7.39 (m, 4H), 2.23 (s, 3H). ^{13}C NMR (101 MHz, d_6 -DMSO) δ (ppm) (major isomer) 166.81, 139.86, 134.30, 128.50, 126.68, 126.44, 125.43, 122.65, 121.96, 121.65, 111.53, 11.96. HRMS (ESI) calculated for $C_{13}H_{13}N_2O_2^+$ $[M + H]^+$ 229.0972, found 229.0949.

B2 is obtained as yellowgreen solid (21% yield). Mp: 132.0 – 134.7 °C. 1H NMR (400 MHz, d_6 -DMSO) δ (ppm) 13.78 (br s, 1H), 13.10 (s, 1H), 7.93 (d, $J = 7.9$ Hz, 1H), 7.81 (d, $J = 8.2$ Hz, 1H), 7.66 – 7.40 (m, 5H), 2.56 (q, $J = 7.4$ Hz, 2H), 1.18 (t, $J = 7.3$ Hz, 3H). ^{13}C NMR (101 MHz, d_6 -DMSO) δ 166.12, 138.73, 134.30, 133.98, 129.09, 127.04, 126.60, 126.35, 121.70, 121.13, 119.67, 107.64, 26.78, 12.33. HRMS (ESI) calculated for $C_{14}H_{15}N_2O_2^+$ $[M + H]^+$ 243.1128, found 243.1121.

B3 is obtained as brown solid (25% yield). Mp: 122.7 – 125.4 °C. 1H NMR (400 MHz, d_6 -DMSO) δ (ppm) 13.81 (br s, 1H), 13.20 (s, 2H), 7.92 (d, $J = 8.1$ Hz, 1H), 7.80 (d, $J = 8.1$ Hz, 1H), 7.66 – 7.42 (m, 5H), 1.64 (dd, $J = 14.9, 7.4$ Hz, 2H), 0.97 (t, $J = 7.4$ Hz, 3H). ^{13}C NMR (101 MHz, d_6 -DMSO) δ 166.27, 138.79, 134.31, 129.07, 127.07, 126.59, 126.31, 121.71, 121.02, 119.74, 107.57, 35.51, 20.97, 14.18. HRMS (ESI) calculated for $C_{15}H_{17}N_2O_2^+$ $[M + H]^+$

+ 257.1285, found 257.1280.

B4 is obtained as green solid (85% yield). Mp: 127.2 – 130.5 °C. ¹H NMR (500 MHz, *d*₆-DMSO) δ (ppm) 13.96 (br s, 1H), 12.65 (s, 1H), 7.92 (s, 1H), 7.79 (s, 1H), 7.58 – 7.49 (m, 5H), 1.33 (s, 9H). ¹³C NMR (101 MHz, *d*₆-DMSO) δ 165.53, 138.78, 138.62, 133.83, 128.59, 126.58, 126.10, 125.81, 121.38, 120.62, 119.31, 107.43, 37.12, 28.81. HRMS (ESI) calculated for C₁₆H₁₉N₂O₂⁺ [M + H]⁺ 271.1441, found 271.1452.

C1 is obtained as white solid (56% yield). Mp: 177.1 – 180.0 °C. ¹H NMR (400 MHz, *d*₆-DMSO) δ (ppm) (Only (*E*)-isomer was detected) 12.12 (br s, 1H), 9.93 (s, 1H), 8.61 (s, 1H), 8.11 (s, 1H), 7.73 (d, *J* = 6.4 Hz, 1H), 7.30 (s, 1H), 2.06 (s, 3H). ¹³C NMR (101 MHz, *d*₆-DMSO) δ 166.11, 141.62, 140.82, 136.09, 123.88, 120.61, 11.63, 0.11. HRMS (ESI) calculated for C₈H₁₀N₃O₂⁺ [M + H]⁺ 180.0768, found 180.0771.

C2 is obtained as yellow solid (24% yield). Mp: 142.2 – 145.6 °C. ¹H NMR (400 MHz, *d*₆-DMSO) (major isomer) δ (ppm) (major isomer) 12.36 (br s, 1H), 10.96 (s, 1H), 8.91 (s, 1H), 8.38 – 8.36 (m, 2H), 7.90 – 7.87 (m, 1H), 2.66 (q, *J* = 7.4 Hz, 2H), 1.04 (t, *J* = 7.6 Hz, 3H). ¹³C NMR (101 MHz, *d*₆-DMSO) δ 165.60, 143.90, 143.02, 134.74, 128.96, 127.87, 127.29, 18.91, 10.61. HRMS (ESI) calculated for C₉H₁₂N₃O₂⁺ [M + H]⁺ 194.0924, found 194.0918.

C3 is obtained as white solid (10% yield). Mp: 149.4 – 152.1 °C. ¹H NMR (400 MHz, *d*₆-DMSO) δ (ppm) (major isomer) 12.01 (br s, 1H), 10.08 (s, 1H), 8.62 (d, *J* = 2.1 Hz, 1H), 8.12 (m, 1H), 7.74 (d, *J* = 8.4 Hz, 1H), 7.32 – 7.29 (m, 1H), 2.59 – 2.41 (m, 2H), 1.51 – 1.45 (m, 2H), 0.96 – 0.92 (m, 3H). ¹³C NMR (101 MHz, *d*₆-DMSO) (major isomer) δ 166.36, 141.96, 141.31, 138.57, 136.41, 124.36, 121.13, 35.45, 19.15, 14.33. HRMS (ESI) calculated for C₁₀H₁₄N₃O₂⁺ [M + H]⁺ 208.1081, found 208.1079.

C4 is obtained as white solid (32% yield). Mp: 130.9 – 136.2 °C. ¹H NMR (500 MHz, *d*₆-DMSO) δ (ppm) 11.03 (s, 1H), 8.49 (s, 1H), 8.11 (s, 1H), 7.68 (s, 1H), 7.38 (s, 1H), 1.25 (d, *J* = 4.8 Hz, 9H). ¹³C NMR (101 MHz, *d*₆-DMSO) δ 165.17, 142.85, 141.68, 139.51, 133.84, 124.56, 121.25, 36.86, 28.51. HRMS (ESI) calculated for C₁₁H₁₆N₃O₂⁺ [M + H]⁺ 222.1237, found 222.1234.

D1 is obtained as yellow solid (78% yield). Mp: 174.0 – 175.3 °C. ¹H NMR (400 MHz, *d*₆-DMSO) δ (ppm) 11.95 (s, 1H), 9.75 (s, 1H), 7.35 (d, *J* = 7.8 Hz, 2H), 7.26 (t, *J* = 7.8 Hz, 2H), 6.88 (t, *J* = 7.2 Hz, 1H), 2.04 (s, 3H). ¹³C NMR (101 MHz, *d*₆-DMSO) δ (ppm) 166.29, 144.36,

132.34, 128.94, 120.77, 113.83, 11.41. HRMS (ESI) calculated for $C_9H_{10}N_2NaO_2^+$ $[M + Na]^+$ 201.0634, found 201.0641.

D2 is obtained as yellow solid (7% yield). Mp: 135.2 – 137.9 °C. 1H NMR (400 MHz, d_6 -DMSO) δ (ppm) (major isomer) 11.87 (s, 1H), 9.91 (s, 1H), 7.34 (d, $J = 7.6$ Hz, 2H), 7.25 (t, $J = 7.6$ Hz, 2H), 6.86 (t, $J = 7.2$ Hz, 2H), 2.57 (q, $J = 7.2$ Hz, 2H), 1.00 (t, $J = 7.6$ Hz, 3H). ^{13}C NMR (101 MHz, d_6 -DMSO) δ (ppm) 166.43, 144.83, 137.36, 129.38, 121.16, 114.25, 18.01, 10.60. HRMS (ESI) calculated for $C_{10}H_{13}N_2O_2^+$ $[M + H]^+$ 193.0972, found 193.0971.

D3 is obtained as yellow solid (50% yield). Mp: 75.9 – 78.5 °C. 1H NMR (400 MHz, d_6 -DMSO) δ (ppm) (major isomer: (*E*)-isomer) 11.85 (br s, 1H), 9.90 (s, 1H), 7.35 (d, $J = 8.0$ Hz, 2H), 7.27 – 7.34 (m, 2H), 6.88 (t, $J = 7.2$ Hz, 1H), 2.57 (t, $J = 7.6$ Hz, 2H), 1.51 – 1.42 (m, 2H), 0.94 (t, $J = 7.2$ Hz, 3H). ^{13}C NMR (101 MHz, d_6 -DMSO) δ (ppm) (major isomer) 166.69, 144.82, 136.25, 129.39, 121.17, 114.27, 35.39, 26.35, 21.00, 19.18, 14.33. HRMS (ESI) calculated for $C_{11}H_{15}N_2O_2^+$ $[M + H]^+$ 207.1128, found 207.1121.

D4 is obtained as yellow solid (74% yield). Mp: 158.4 – 161.7 °C. 1H NMR (500 MHz, d_6 -DMSO) δ (ppm) 13.60 (s, 1H), 11.34 (s, 1H), 7.25 (t, $J = 7.7$ Hz, 2H), 7.17 (d, $J = 7.8$ Hz, 2H), 6.86 (t, $J = 7.1$ Hz, 1H), 1.26 (s, 9H). ^{13}C NMR (101 MHz, d_6 -DMSO) δ (ppm) 165.45, 144.79, 137.97, 129.63, 121.11, 113.60, 37.26, 29.21. HRMS (ESI) calculated for $C_{12}H_{15}N_2O_2^-$ $[M-H]^-$ 219.1139, found 219.1131.

4.9 Antimicrobial susceptibility testing

Susceptibility testing was performed by broth microdilution assay according to Clinical and Laboratory Standards Institute (CLSI) methods (CLSI M07-A9). Briefly, fresh bacterial overnight colony growth was resuspended in sterile saline, adjusted to a cell density of about 1×10^8 colony-forming units (CFU)/mL. Then the liquid was diluted by Mueller-Hinton Broth and transferred 100 μ L to the wells, with the final target inoculum of about 5×10^5 CFU/mL. Tested compounds were prepared in 100% DMSO with the stock concentration of 20 mg/mL. The compounds were added to the wells with final compound concentration of 100 μ g/mL. The two-fold diluted final concentrations of meropenem were 64 to 0.0625 μ g/mL. Assay microtiter plates were incubated for 20 – 24 hours at 37°C. Following incubation, assay plates were monitored for bacterial growth. The minimal inhibitory concentration (MIC) is defined as the

lowest concentration of antibiotic at which the visible growth of the organism is completely inhibited.

Appendix A. Supplementary data

Chemical shift perturbations of NDM-1 observed by NMR spectroscopy. NMR spectra of compounds in this study. Analytical HPLC trace for compounds in this study.

Acknowledgements

We gratefully acknowledge the grants from the National Natural Science Foundation of China (81703418, 21575156) and the CAMS Innovation Fund for Medical Sciences (CIFMS, 2017-I2M-1-012).

References

- [1] L. S. J. Roope, R. D. Smith, K. B. Pouwels, J. Buchanan, L. Abel, P. Eibich, C. C. Butler, P. S. Tan, A. S. Walker, J. V. Robotham, S. Wordsworth, The challenge of antimicrobial resistance: what economics can contribute. *Science*. 364(6435) (2019) pii: eaau4679.
- [2] M. Hancock, "Antimicrobial resistance needs an urgent global response" (speech given at World Economic Forum in Davos, 24 January 2019); www.gov.uk/government/speeches/antimicrobial-resistance-needs-an-urgent-global-response.
- [3] World Health Organization, Global priority list of antibiotic-resistant bacteria to guide research, discovery, and development of new antibiotics. Feb 27th, 2017.
- [4] E. Tacconelli, E. Carrara, A. Savoldi, S. Harbarth, M. Mendelson, D. L. Monnet, C. Pulcini, G. Kahlmeter, J. Kluytmans, Y. Carmeli, M. Ouellette, K. Outterson, J. Patel, M. Cavaleri, E. M. Cox, C. R. Houchens, M. L. Grayson, P. Hansen, N. Singh, U. Theuretzbacher, N. Magrini, and the WHO Pathogens Priority List Working Group, Discovery, research, and development of new antibiotics: the WHO priority list of antibiotic-resistant bacteria and tuberculosis. *Lancet. Infect. Dis.* 18 (2018) 318-327.
- [5] F. S. Codjoe, E. S. Donkor, Carbapenem resistance: a review. *Med. Sci. (Basel)*. 6 (2017) pii: E1.
- [6] G. Meletis, Carbapenem resistance: overview of the problem and future perspectives. *Ther. Adv. Infect. Dis.* 3 (2016) 15-21.
- [7] M. I. El-Gamal, I. Brahim, N. Hisham, R. Aladdin, H. Mohammed, A. Bahaaeldin, Recent updates of carbapenem antibiotics. *Eur. J. Med. Chem.* 131 (2017) 185-195.

- [8] G. Cornaglia, H. Giamarellou, G. M. Rossolini, Metallo- β -lactamases: a last frontier for β -lactams? *Lancet. Infect. Dis.* 11 (2011) 381-393.
- [9] D. Yong, M. A. Toleman, C. G. Giske, H. S. Cho, K. Sundman, K. Lee, T. R. Walsh, Characterization of a new metallo-beta-lactamase gene, bla(NDM-1), and a novel erythromycin esterase gene carried on a unique genetic structure in *Klebsiella pneumoniae* sequence type 14 from India. *Antimicrob. Agents. Chemother.* 53 (2009) 5046-5054.
- [10] P. Linciano, L. Cendron, E. Gianquinto, F. Spyraakis, D. Tondi, Ten years with New Delhi Metallo- β -lactamase-1 (NDM-1): from structural insights to inhibitor design. *ACS Infect. Dis.* 5 (2019) 9-34.
- [11] S. M. Drawz, R. A. Bonomo, Three decades of beta-lactamase inhibitors. *Clin. Microbiol. Rev.* 23 (2010) 160-201.
- [12] K. Bush, P. A. Bradford, β -Lactams and β -lactamase inhibitors: an overview. *Cold. Spring. Harb. Perspect. Med.* 6 (2016) pii: a025247.
- [13] Y. Guo, J. Wang, G. Niu, W. Shui, Y. Sun, H. Zhou, Y. Zhang, C. Yang, Z. Lou, Z. Rao, A structural view of the antibiotic degradation enzyme NDM-1 from a superbug. *Protein Cell.* 2 (2011) 384-394.
- [14] N. Li, Y. Xu, Q. Xia, C. Bai, T. Wang, L. Wang, D. He, N. Xie, L. Li, J. Wang, H. G. Zhou, F. Xu, C. Yang, Q. Zhang, Z. Yin, Y. Guo, Y. Chen, Simplified captopril analogues as NDM-1 inhibitors. *Bioorg. Med. Chem. Lett.* 24 (2014) 386-389.
- [15] D. T. King, L. J. Worrall, R. Gruninger, N. C. Strynadka, New Delhi metallo- β -lactamase: structural insights into β -lactam recognition and inhibition. *J. Am. Chem. Soc.* 134 (2012) 11362-11365.
- [16] C. Yao, Q. Wu, G. Xu, C. Li, NMR backbone resonance assignment of New Delhi metallo-beta-lactamase. *Biomol. NMR Assign.* 11 (2017) 239-242.
- [17] J. Brem, R. Cain, S. Cahill, M. A. McDonough, I. J. Clifton, J. C. Jiménez-Castellanos, M. B. Avison, J. Spencer, C. W. Fishwick, C. J. Schofield, Structural basis of metallo- β -lactamase, serine- β -lactamase and penicillin-binding protein inhibition by cyclic boronates. *Nat. Commun.* 7 (2016) 12406.
- [18] M. M. González, M. Kosmopoulou, M. F. Mojica, V. Castillo, P. Hinchliffe, I. Pettinati, J. Brem, C. J. Schofield, G. Mahler, R. A. Bonomo, L. I. Llarrull, J. Spencer, A. J. Vila, Bisthiazolidines: a substrate-mimicking scaffold as an inhibitor of the NDM-1 carbapenemase. *ACS Infect. Dis.* 1 (2015) 544-554.
- [19] J. Zhang, S. Wang, Q. Wei, Q. Guo, Y. Bai, S. Yang, F. Song, L. Zhang, X. Lei, Synthesis and biological evaluation of aspergillomarasmine A derivatives as novel NDM-1 inhibitor to overcome antibiotics resistance. *Bioorg. Med. Chem.* 25 (2017) 5133-5141.

- [20] T. Christopheit, A. Albert, H. S. Leiros, Discovery of a novel covalent non- β -lactam inhibitor of the metallo- β -lactamase NDM-1. *Bioorg. Med. Chem.* 24 (2016) 2947-2953.
- [21] F. M. Klingler, T. A. Wichelhaus, D. Frank, J. Cuesta-Bernal, J. El-Delik, H. F. Müller, H. Sjuts, S. Göttig, A. Koenigs, K. M. Pos, D. Pogoryelov, E. Proschak, Approved drugs containing thiols as inhibitors of metallo- β -lactamases: strategy to combat multidrug-resistant bacteria. *J. Med. Chem.* 58 (2015) 3626-3630.
- [22] L. Zhai, Y. L. Zhang, J. S. Kang, P. Oelschlaeger, L. Xiao, S. S. Nie, K. W. Yang, Triazolylthioacetamide: a valid scaffold for the development of new delhi metallo- β -lactamase-1 (NDM-1) inhibitors. *ACS Med. Chem. Lett.* 7 (2016) 413-417.
- [23] V. Yarlagadda, P. Sarkar, S. Samaddar, G. B. Manjunath, S. D. Mitra, K. Paramanandham, B. R. Shome, J. Haldar, Vancomycin analogue restores meropenem activity against NDM-1 gram-negative pathogens. *ACS Infect. Dis.* 4 (2018) 1093-1101.
- [24] A. Krajnc, J. Brem, P. Hinchliffe, K. Calvopiña, T. D. Panduwawala, P. A. Lang, J. J. A. G. Kamps, J. M. Tyrrell, E. Widlake, B. G. Saward, T. R. Walsh, J. Spencer, C. J. Schofield, Bicyclic Boronate VNRX-5133 Inhibits Metallo- and Serine- β -Lactamases. *J. Med. Chem.* 62 (2019) 8544-8556.
- [25] H. Meredith, D. S., Antimicrobial Activity of Cefepime in Combination with VNRX-5133 Against a Global 2018 Surveillance Collection of Clinical Isolates; European Congress of Clinical Microbiology and Infectious Diseases (ECCMID) in Amsterdam: The Netherlands (2019).
- [26] A. Piccirilli, B. Segatore, D. Daigle, G. Amicosante, M. Perilli, VNRX-5133 maintains potent inhibitory activity in engineered NDM-1 variants with increased cefepime hydrolytic efficiency. European Congress of Clinical Microbiology and Infectious Diseases (ECCMID) in Amsterdam: The Netherlands (2019).
- [27] X. Wang, M. Lu, Y. Shi, Y. Ou, X. Cheng, Discovery of novel New Delhi Metallo- β -Lactamases-1 inhibitors by multistep virtual screening. *PLoS One.* 10 (2015) e0118290.
- [28] J. S. Kang, A. L. Zhang, M. Faheem, C. J. Zhang, N. Ai, J. D. Buynak, W. J. Welsh, P. Oelschlaeger, Virtual screening and experimental testing of B1 Metallo- β -lactamase inhibitors. *J. Chem. Inf. Model.* 58 (2018) 1902-1914.
- [29] F. Spyrakis, G. Celenza, F. Marcocchia, M. Santucci, S. Cross, P. Bellio, L. Cendron, M. Perilli, D. Tondi, Structure-based virtual screening for the discovery of novel inhibitors of New Delhi Metallo- β -lactamase-1. *ACS Med. Chem. Lett.* 9 (2018) 45-50.
- [30] C. Shi, J. Bao, Y. Sun, X. Kang, X. Lao, H. Zheng, Discovery of baicalin as NDM-1 inhibitor: virtual screening, biological evaluation and molecular simulation. *Bioorg. Chem.* 88 (2019) 102953.

- [31] C. Shi, J. Chen, B. Xiao, X. Kang, X. Lao, H. Zheng, Discovery of NDM-1 inhibitors from natural products. *J. Glob. Antimicrob. Resist.* 18 (2019) 80-87.
- [32] P. K. Thakur, J. Kumar, D. Ray, F. Anjum, M. I. Hassan, Search of potential inhibitor against New Delhi metallo-beta-lactamase 1 from a series of antibacterial natural compounds. *J. Nat. Sci. Biol. Med.* 4 (2013) 51-56.
- [33] A. U. Khan, A. Ali, Danishuddin, G. Srivastava, A. Sharma, Potential inhibitors designed against NDM-1 type metallo- β -lactamases: an attempt to enhance efficacies of antibiotics against multi-drug-resistant bacteria. *Sci. Rep.* 7 (2017) 9207.
- [34] M. T. Rehman, M. F. AlAjmi, A. Hussain, G. M. Rather, M. A. Khan. High-throughput virtual screening, molecular dynamics simulation, and enzyme kinetics identified ZINC84525623 as a potential inhibitor of NDM-1. *Int J Mol Sci.* 20 (2019) pii: E819.
- [35] D. Rogolino, M. Carcelli, M. Sechi, N. Neamati, Viral enzymes containing magnesium: metal binding as a successful strategy in drug design. *Coord. Chem. Rev.* 256 (2012) 3063–3086.
- [36] D. P. Martin, P. G. Blachly, J. A. McCammon, S. M. Cohen, Exploring the influence of the protein environment on metal-binding pharmacophores. *J. Med. Chem.* 57 (2014) 7126-7135.
- [37] J. A. Jacobsen, J. L. Fullagar, M. T. Miller, S. M. Cohen, Identifying chelators for metalloprotein inhibitors using a fragment-based approach. *J. Med. Chem.* 54 (2011) 591-602.
- [38] C. A. Lipinski, F. Lombardo, B. W. Dominy, P. J. Feeney, Experimental and computational approaches to estimate solubility and permeability in drug discovery and development settings. *Adv. Drug. Deliv. Rev.* 23 (1997) 3-25.
- [39] D. F. Veber, S. R. Johnson, H. Y. Cheng, B. R. Smith, K. W. Ward, K. D. Kopple, Molecular properties that influence the oral bioavailability of drug candidates. *J. Med. Chem.* 45 (2002) 2615-2623.
- [40] U. H. Danielson, Fragment library screening and lead characterization using SPR biosensors. *Curr. Top. Med. Chem.* 9 (2009) 1725-1735.
- [41] T. Christopheit, H. K. Leiros, Fragment-based discovery of inhibitor scaffolds targeting the metallo- β -lactamases NDM-1 and VIM-2. *Bioorg. Med. Chem. Lett.* 26 (2016) 1973-1977.
- [42] A. Bax, G. M. Clore, Protein NMR: Boundless opportunities. *J. Magn. Reson.* pii: S1090-7807 (2019) 30150-30158.
- [43] H. Arthanari, K. Takeuchi, A. Dubey, G. Wagner, Emerging solution NMR methods to illuminate the structural and dynamic properties of proteins. *Curr. Opin. Struct. Biol.* 52 (2019) 1-11.

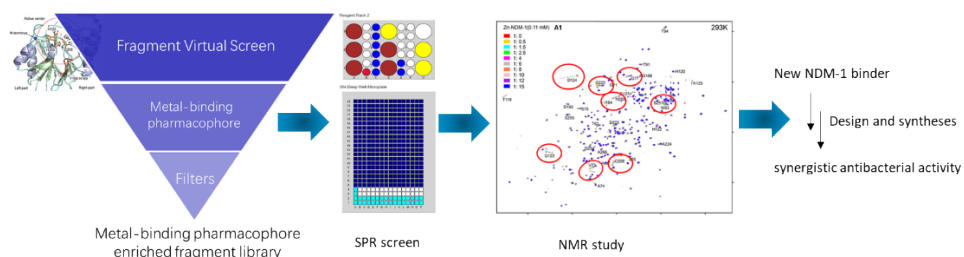
- [44] H. Feng, J. Ding, D. Zhu, X. Liu, X. Xu, Y. Zhang, S. Zang, D. C. Wang, W. Liu, Structural and mechanistic insights into NDM-1 catalyzed hydrolysis of cephalosporins. *J. Am. Chem. Soc.* 136 (2014) 14694-14697.
- [45] R. A. Taylor, N. M. Bonanno, D. Mirza, A. J. Lough, M. T. Lemaire, A trivalent cobalt complex with the new redox-active ligand 10-(8-quinolylazo)-9-phenanthrol (qap). *Polyhedron*. 131 (2017) 34-39.
- [46] J. W. Lyga, A Convenient synthesis of 1-aryl- Δ^2 -1,2,4-triazolin-5-ones from arylhydrazines. *Synthetic Commun.* 16 (1986) 163-167.
- [47] No author. Captopril approved for hypertension. *FDA Drug Bull.* 11 (1981) 10-11.
- [48] M. F. Richter, B. S. Drown, A. P. Riley, A. Garcia, T. Shirai, R. L. Svec, P. J. Hergenrother. Predictive compound accumulation rules yield a broad-spectrum antibiotic. *Nature*. 545(2017) 299-304.
- [49] R. O'Shea, H. E. Moser, Physicochemical properties of antibacterial compounds: implications for drug discovery. *J. Med. Chem.* 51(2008) 2871-2878.
- [50] A. Y. Chen, R. N. Adamek, B. L. Dick, C. V. Credille, C. N. Morrison, S. M. Cohen, Targeting metalloenzymes for therapeutic intervention. *Chem. Rev.* 119 (2019) 1323-1455.

Declaration of interests

The authors declare that they have no known competing financial interests or personal relationships that could have appeared to influence the work reported in this paper.

The authors declare the following financial interests/personal relationships which may be considered as potential competing interests:

Journal Pre-proofs



A novel scaffold of NDM-1 inhibitors is described. The scaffold was discovered from metal-binding pharmacophore enriched library with virtual and SPR screen. Solution NMR found that the scaffold binds to the NDM-1 active pocket and the zinc ion in the pocket. Design and syntheses found compounds with synergistic antibacterial activity.